J. Fluid Mech. (2006), *vol.* 547, *pp.* 1–20. © 2006 Cambridge University Press 1
doi:10.1017/S002211200500697X Printed in the United Kingdom

Linear stability of spiral and annular Poiseuille flow for small radius ratio

By DAVID L. COTRELL† AND ARNE J. PEARLSTEIN

Department of Mechanical and Industrial Engineering, University of Illinois at Urbana-Champaign, 1206 West Green Street, Urbana, IL 61801, USA

(Received 27 February 2004 and in revised form 1 June 2005)

For the radius ratio $\eta \equiv R_i/R_o = 0.1$ and several rotation rate ratios $\mu \equiv \Omega_o/\Omega_i$, we consider the linear stability of spiral Poiseuille flow (SPF) up to $Re = 10^5$, where R_i and R_o are the radii of the inner and outer cylinders, respectively, $Re \equiv \overline{V}_Z(R_o - R_i)/\nu$ is the Reynolds number, Ω_i and Ω_o are the (signed) angular speeds of the inner and outer cylinders, respectively, ν is the kinematic viscosity, and $\overline{V}_Z$ is the mean axial velocity. The Re range extends more than three orders of magnitude beyond that considered in the previous $\mu = 0$ work of Recktenwald *et al.* (*Phys. Rev.* E, vol. 48, 1993, p. 444). We show that in the non-rotating limit of annular Poiseuille flow, linear instability does not occur below a critical radius ratio $\hat{\eta} \approx 0.115$. We also establish the connection of the linear stability of annular Poiseuille flow for $0 < \eta \leqslant \hat{\eta}$ at all Re to the linear stability of circular Poiseuille flow ($\eta = 0$) at all Re. For the rotating case, with $\mu = -1, -0.5, -0.25, 0$ and 0.2, the stability boundaries, presented in terms of critical Taylor number $Ta \equiv \Omega_i(R_o - R_i)^2/\nu$ versus Re, show that the results are qualitatively different from those at larger η. For each μ, the centrifugal instability at small Re does not connect to a high-Re Tollmien–Schlichting-like instability of annular Poiseuille flow, since the latter instability does not exist for $\eta < \hat{\eta}$. We find a range of Re for which disconnected neutral curves exist in the k–Ta plane, which for each non-zero μ considered, lead to a multi-valued stability boundary, corresponding to two disjoint ranges of stable Ta. For each counter-rotating ($\mu < 0$) case, there is a finite range of Re for which there exist three critical values of Ta, with the upper branch emanating from the $Re = 0$ instability of Couette flow. For the co-rotating ($\mu = 0.2$) case, there are two critical values of Ta for each Re in an apparently semi-infinite range of Re, with neither branch of the stability boundary intersecting the $Re = 0$ axis, consistent with the classical result of Synge that Couette flow is stable with respect to all small disturbances if $\mu > \eta^2$, and our earlier results for $\mu > \eta^2$ at larger η.

1. Introduction

The stability of spiral Poiseuille flow (SPF) between coaxial cylinders, driven by rotation of one or both cylinders and an axial pressure gradient, has been of interest for many years (Takeuchi & Jankowski 1981; Ng & Turner 1982; Meseguer & Marques 2002). Cotrell & Pearlstein (2004) and Cotrell, Rani & Pearlstein (2004), hereinafter referred to as CP and CRP, respectively, have presented complete linear stability boundaries for several radius ratios and rotation rate ratios, identified the connection between centrifugal instability when there is no axial flow and a Tollmien–Schlichting-like

† Present address: Lawrence Livermore National Laboratory, P.O. Box 808, Livermore, CA 94551, USA.

instability of non-rotating annular Poiseuille flow, and showed that the computed stability boundaries are in excellent agreement with experiment over wide ranges of Re and the ratio of the angular velocities of the two cylinders.

The wide-gap case is of significant potential interest in applications, since, with no mean axial flow, the stable range $Ta_1 \leqslant Ta \leqslant Ta_2$ for steady axisymmetric Taylor vortex flow increases as η decreases (Debler, Füner & Schaaf 1969; Snyder 1970; DiPrima, Eagles & Ng 1984), with Ta_2/Ta_1 seeming to be between 10 and 100 for $\eta = 0.5$, compared to much smaller values in the narrow-gap ($\eta \rightarrow 1$) limit. Here, $\eta \equiv R_i/R_o$ is the radius ratio, $Ta \equiv \Omega_i(R_o - R_i)^2/\nu$ is the Taylor number, R_i and R_o are the radii of the inner and outer cylinders, respectively, Ω_i and ν are the angular speed of the inner cylinder and the kinematic viscosity, respectively, and Ta_1 and Ta_2 are the critical values at which steady Couette flow and steady Taylor vortex flow, respectively, lose their stability. If axially-propagating axisymmetric Taylor-like vortices remain stable in a large range of Ta when a small mean axial pressure gradient is superimposed, then flow in a wide-gap or small-η annulus driven by cylinder rotation and an axial pressure gradient will be of interest where laminar (and particularly, steady and axisymmetric) heat or mass transfer at rates in excess of the diffusive rate associated with Couette flow is desired. The laminar nature of the flow is especially important for mixing in a number of biomedical and biotechnology applications, where turbulent shear is associated with cell damage (Strong & Carlucci 1976; Resende *et al.* 2001).

To date, the only published results for the stability of SPF with $\eta < 0.5$ appear to be those of Chung & Astill (1977), Hasoon & Martin (1977), and Recktenwald, Lücke & Müller (1993), all of which are restricted to $\mu \equiv \Omega_o/\Omega_i = 0$, where Ω_o is the angular speed of the outer cylinder. Chung & Astill graphically showed critical values of Ta for $Re = 0$, 50 and 100 at $\eta = 0.1$ and 0.25, and for $Re = 150$ at $\eta = 0.25$. (Here, $Re \equiv \overline{V}_Z(R_o - R_i)/\nu$ is the Reynolds number, where $\overline{V}_Z$ is the mean axial speed. We have converted other authors' Reynolds numbers to values based on our definition.) As discussed in § 3.1, their numerical results are incorrect. Contemporaneously, Hasoon & Martin (1977) reported computations of the critical Taylor number up to $Re = 1000$. They used an axial velocity profile uniform across the annular cross-section, which approximation was said to be validated by comparison to results at $\eta = 0.9$ for the correct axial profile. The correctness of the results of Hasoon & Martin has been questioned by DiPrima & Pridor (1979), who also identified an error in the governing equations used by the former authors. In Recktenwald *et al.* (1993), $\eta = 0.1$ was one of the radius ratios for which the stability of SPF with respect to axisymmetric disturbances was investigated numerically over the range $0 \leqslant Re \leqslant 20$, and for which a quadratic function of Re^2 was fitted to the results.

Here, we report SPF stability computations for $\eta = 0.1$. For the five values of μ investigated, the Reynolds-number range extends more than three orders of magnitude beyond the largest Re considered in the $\mu = 0$ analysis of Recktenwald *et al.* (1993). For $\mu \neq 0$, the results at small and intermediate Re differ qualitatively from their results at $\mu = 0$, and also from ours (CP, CRP) at larger η. For both positive and negative values of μ, we find regions of Re in which closed neutral curves give rise to two disjoint ranges of stable Ta. We also show that annular Poiseuille flow ($Ta = 0$) is linearly stable for all Re if $\eta < \hat{\eta} \approx 0.115$, so that at high Re there is no transition from centrifugal instability to a Tollmien–Schlichting-like instability, unlike the larger-η cases previously studied.

The paper is organized as follows. The results are presented in § 2, followed by a discussion in § 3 of the relationship to other work, the direction of disturbance

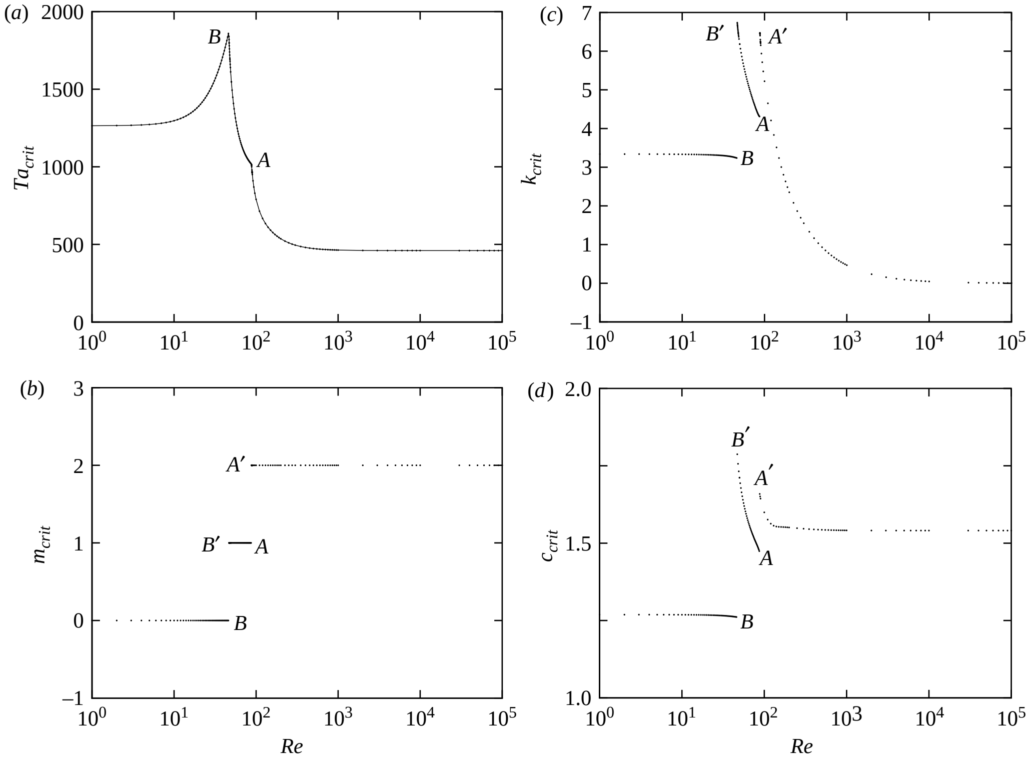

FIGURE 1. For $\mu = 0$ and $\eta = 0.1$: (*a*) critical *Ta*, (*b*) critical *m*, (*c*) critical *k*, (*d*) critical *c* versus *Re*.

wave propagation, and implications for experiment. Some conclusions are presented in § 4.

2. Results

The formulation and numerical methods are discussed in CP. Code validation was accomplished by comparison to previous tabulated results for $\eta \geqslant 0.5$, as described in CP. Comparison of computations at smaller η to the graphical results of Mahadevan & Lilley (1977) and Garg (1980) for annular Poiseuille flow ($Ta = 0$), and to the tabulated small-*Re* results of Recktenwald *et al.* (1993) (see § 3.1) revealed excellent agreement. In contrast to the 40 terms that always provided adequate resolution convergence for larger η (CP), up to 70 terms were sometimes required to achieve convergence for $\eta = 0.1$.

We present results for cases in which the outer cylinder is fixed ($\mu = 0$), or rotates in the opposite direction to ($\mu = -0.25$, -0.5 and -1) or in the same direction as ($\mu = 0.2$) the inner cylinder. Results for three of these rotation rate ratios ($\mu = -0.5$, 0 and 0.2) have been presented for $\eta = 0.5$ by Takeuchi & Jankowski (1981) and in CP, and allow the effects of smaller radius ratio to be clearly identified. The other two counter-rotating cases ($\mu = -1$ and -0.25) provide additional information on the effects of the rotation rate ratio on the stability of counter-rotating flow.

2.1. *Non-rotating outer cylinder*

For $\mu = 0$, critical values of the Taylor number *Ta*, azimuthal wavenumber *m*, dimensionless axial wavenumber *k*, and dimensionless wave speed *c* are shown in figure 1.

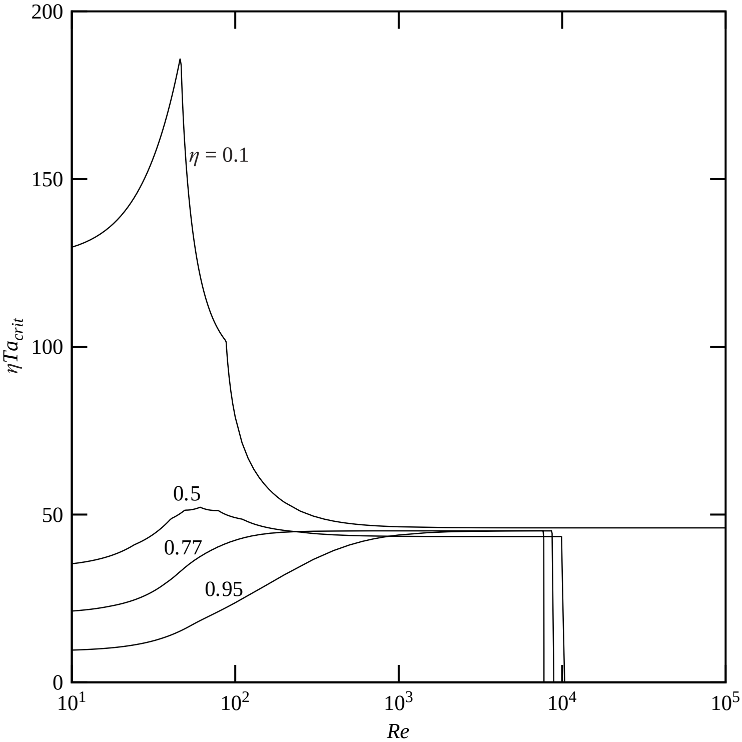

FIGURE 2. Critical ηTa versus Re for $\mu = 0$ and $\eta = 0.1$, 0.5, 0.77 and 0.95.

(The dimensionless axial wavenumber and wave speed are scaled with the gap and mean axial velocity, respectively, as discussed in CP.). Figure 1(a) shows that the stability boundary is a single-valued function of Re (i.e. there is a single critical Ta for each Re). For all combinations of μ and η satisfying $\mu < \eta^2$ considered in CP and CRP, the stability boundary was single-valued for $0 \leqslant Re \leqslant Re_{AP}(\eta)$, with the flow unstable at all Ta for $Re > Re_{AP}$, where Re_{AP} is the critical Re for annular Poiseuille flow. For $\eta = 0.1$, the $Re = 0$ intercept of the stability boundary at $Ta_{crit} = 1264.43$ corresponds to the onset of Taylor vortex flow. As Re increases, Ta_{crit} increases until reaching a global maximum (near $Re = 46$). As for larger η, scalloping occurs due to integer jumps in m_{crit}, with the pronounced slope discontinuities near $Re = 46$ (point B) and 87 (point A) corresponding to transitions of the critical azimuthal wavenumber (m_{crit}) from 0 to 1, and from 1 to 2, respectively. As Re increases beyond the maximum at 46, Ta_{crit} decreases and approaches an asymptotic value $Ta_{crit}^{\infty} \approx 460$.

As shown in figure 2, this result differs qualitatively from results at larger η (CP and CRP), for which Ta_{crit} decreases sharply at Re^*, corresponding to transition from a centrifugal instability to a Tollmien–Schlichting-like instability. The $\eta = 0.1$ behaviour is consistent with that reported for the non-rotating ($Ta = 0$) annular Poiseuille case at small η by Mahadevan & Lilley (1977) and Garg (1980), who found that Re_{AP} increases rapidly as η decreases below 0.15. For $Ta = 0$, table 1 shows that as η decreases below 0.2, Re_{AP} increases monotonically, and that there appears to be a critical value $\hat{\eta} < 0.12$ below which no critical Re_{AP} exists. Extrapolation of linear and quadratic least-squares polynomials fitted to the η dependence of $1/Re_{AP}$ for the three and four smallest values of η for which Re_{AP} was computed gives values of

η	Re_{crit}	k_{crit}	m_{crit}	c_{crit}
0.12	205 486	0.20038	1	0.289
0.125	107 424	0.32219	1	0.304
0.13	72 665	0.41182	1	0.318
0.133	60 328	0.45830	1	0.326
0.135	53 986	0.48739	1	0.331
0.137	48 710	0.51524	1	0.336
0.14	42 286	0.55488	1	0.344
0.15	28 660	0.67428	1	0.366
0.16	21 277	0.77912	1	0.385
0.17	16 900	0.87593	1	0.400
0.18	14 170	0.95879	1	0.412
0.19	12 432	1.0331	1	0.421
0.2	11 326	1.0988	1	0.426
0.3	11 475	1.4350	1	0.393
0.4	14 552	1.6307	1	0.354
0.5	10 359	1.4786	2	0.404
0.6	10 296	1.7175	2	0.385
0.77	8883.3	1.9974	1	0.383
0.8	8548.4	2.0204	0	0.386
0.95	7739.5	2.0399	0	0.395

TABLE 1. Critical values versus η for annular Poiseuille flow.

$\hat{\eta}=0.1145$ and 0.1143, respectively. Nonlinear least-squares fitting of the results to a curve of the form $Re=a(\eta-\eta_o)^b$ gives $\eta_o=0.1145$, 0.1142, 0.1156 and 0.1156, using values at the three, four, five and six smallest values of η, respectively. This suggests a critical radius ratio of about 0.115 below which annular Poiseuille flow is linearly stable for all Re.

Figure 3 shows neutral curves in the k–Ta plane for several azimuthal wavenumbers. Neutral curves for $m=1$ and 2 each consist of a single 'primary' neutral curve (not displayed, since they lie far above the Ta range shown) and one closed disconnected neutral curve (CDNC). Each primary neutral curve has a vertical asymptote at $k=0$, with Ta tending to infinity as $k\rightarrow\infty$. The closed neutral curves are said to be disconnected in the sense that they are not connected to other neutral curves at bifurcation points (Pearlstein 1981; Pearlstein, Harris & Terrones 1989). For values of m other than 1 and 2, there is only a primary neutral curve. In contrast to results for larger η (cf. figure 4 of Ng & Turner 1982), the primary neutral curves for some m (e.g. $m=0$) are the 'envelopes' of two intersecting branches, across each of which one temporal eigenvalue (or possibly a pair) crosses into the right half-plane (RHP). At the intersections, the slopes of these primary neutral curves are discontinuous. The parts of these branches not shown (i.e. the smooth continuation of each branch through the junction) correspond to curves on which one or more additional eigenvalues cross into the RHP, in addition to the one that crossed at a lower Ta on the primary branch. For $\mu=0$, figure 3 shows that existence of CDNCs in the k–Ta plane does not lead to multiple ranges of stable Ta for fixed Re. For a CDNC to lead to a multi-valued stability boundary, either there must be no primary neutral curve (as for $\eta=0.5$ and $\mu>\eta^2$ in CP), or there must be some range of Ta lying between the maximum Ta on a CDNC and the minimum Ta on a primary neutral curve, through which no other neutral curve passes. For $\eta=0.1$, neither situation obtains for $\mu=0$.

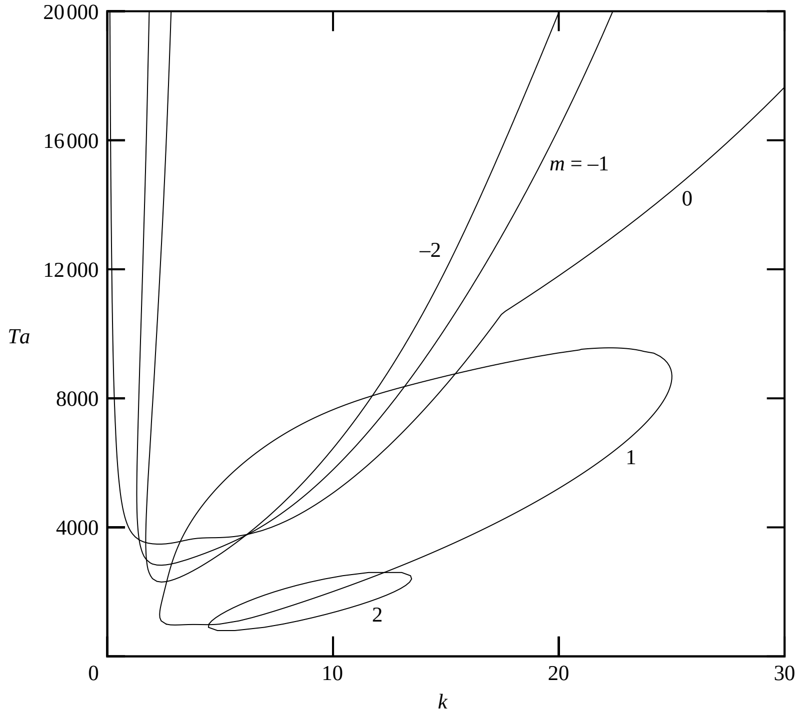

FIGURE 3. Neutral curves for $Re = 100$, $\mu = 0$ and $\eta = 0.1$.

Figure 1(*b*) shows that m_{crit} increases stepwise, from 0 for $0 \leqslant Re \leqslant 46$, to 1 for $46 \leqslant Re \leqslant 87$, and to 2 for $Re \geqslant 87$. The value of m_{crit} remains 2 up to at least $Re = 10^5$.

As is the case for $\eta = 0.5$ (Takeuchi & Jankowski 1981; CP), figure 1(*c*) shows that k_{crit} is a piecewise continuous function of Re, and decreases monotonically with increasing Re over each range for which m_{crit} is a constant. This behaviour leads to the three-part 'wavenumber fan' shown. To an excellent degree of approximation, k_{crit} varies inversely with Re over the range $250 \leqslant Re \leqslant 10^5$.

Figure 1(*d*) shows that the dimensionless wave speed of the critical disturbance, c_{crit}, which is the ratio of the dimensional phase velocity to the mean axial speed $\overline{V}_Z$, is nearly constant over the range of Re for which $m_{crit} = 0$. Near $Re = 46$, where m_{crit} increases from 0 to 1, c_{crit} jumps by about 50 %, and then falls over the range where $m_{crit} = 1$. It then increases discontinuously again near $Re = 87$, where m_{crit} jumps to 2. The critical wave speed approaches an asymptotic value of about 1.54 as $Re \to \infty$.

2.2. *Counter-rotating cylinders* ($\mu < 0$)

For $\mu = -0.25$, -0.5 and -1, the results differ qualitatively from those for $\mu = 0$ (§ 2.1), and from those for $\mu = -0.5$ at $\eta \geqslant 0.5$ (Takeuchi & Jankowski 1981; CP; CRP). We discuss the three values of μ in order, with a detailed description of the neutral curves being given for $\mu = -0.5$, the counter-rotating case studied at larger η.

$\mu = -0.25$

For $\mu = -0.25$, figure 4(*a*) shows that over the range $0 \leqslant Re \leqslant 94$, Ta_{crit} is single-valued and decreases monotonically from its value of 2759.3 at $Re = 0$. Near $Re = 60$ (point *B*), the slope on the high-*Ta* branch changes discontinuously, corresponding

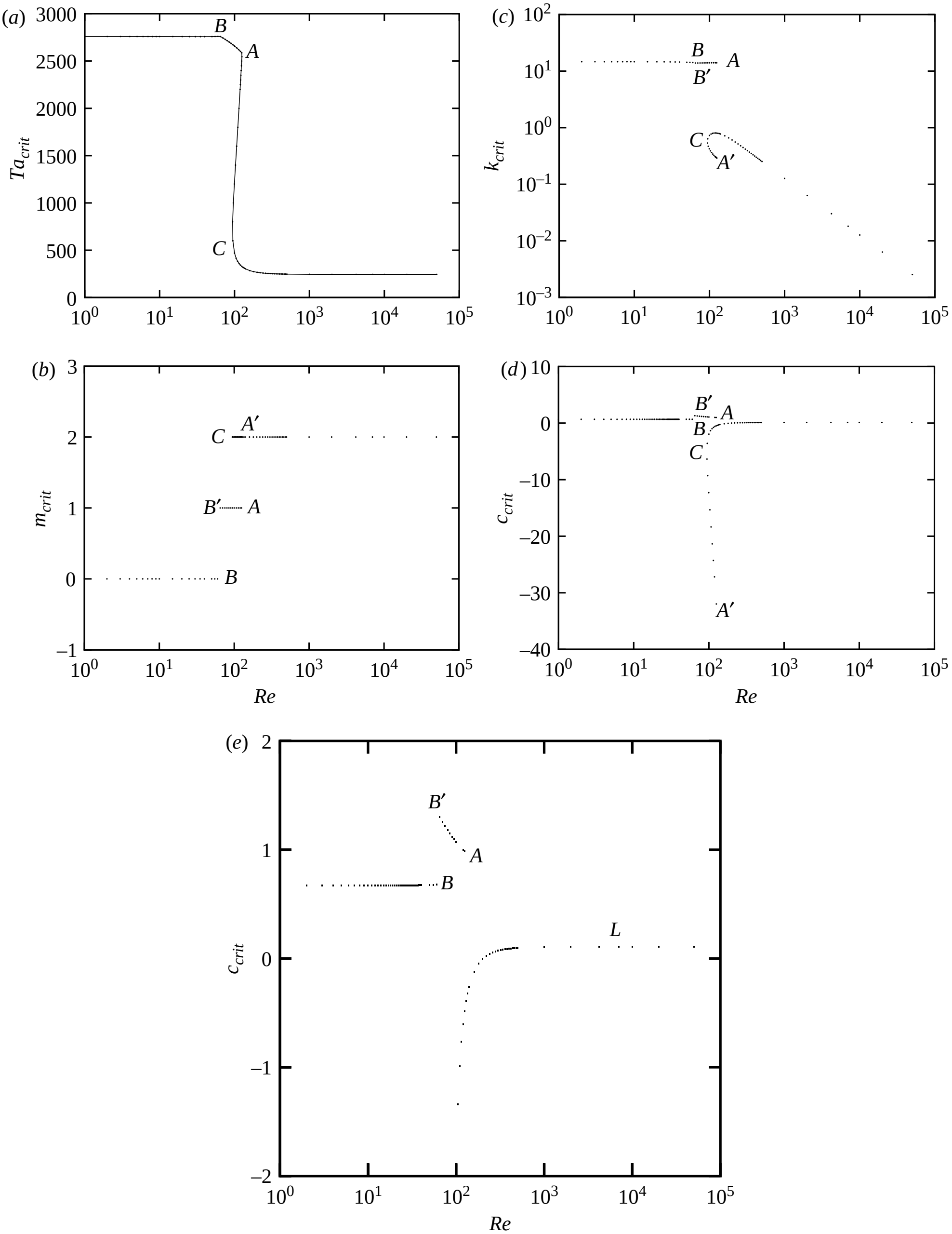

FIGURE 4. For $\mu = -0.25$ and $\eta = 0.1$: (*a*) critical *Ta*, (*b*) critical *m*, (*c*) critical *k*, (*d*) critical *c* versus *Re*, (*e*) Enlargement of part of (*d*).

to m_{crit} increasing from 0 to 1, as shown in figure 4(*b*). More strikingly, for $94 < Re \leqslant 125.5$, there exist three values of Ta_{crit} and two disjoint ranges of stable *Ta*, one below the low-*Ta* branch and one between the intermediate- and high-*Ta* branches. A second slope discontinuity occurs where the high-*Ta* (low-*Re*) branch joins the intermediate branch near $Re = 125.5$ (point *A*). The intermediate-*Ta* branch continues downward to the turning point *C*, where it smoothly connects with the low-Ta (high-Re) branch at $Re = 95$. For large Re, Ta_{crit} approaches an asymptotic value $Ta_{crit}^{\infty} \approx 244$.

This triple-valued stability boundary is a direct consequence of the existence of CDNCs, previously found in stability analyses of quiescent fluid layers in which the density depends on two or more stratifying agencies with different diffusivities (Pearlstein 1981; Pearlstein *et al.* 1989; Terrones & Pearlstein 1989; Lopez, Romero & Pearlstein 1990), in a buoyancy-driven flow in an inclined layer (Chen & Pearlstein 1989), in differentially rotating flows between differentially heated concentric vertical cylinders (Ali & Weidman 1990) and in a two-phase parallel shear flow with a deformable interface (Blennerhassett 1980). This will be illustrated in detail below for $\mu = -0.5$, a case in which the range of triple-valuedness is larger. As discussed for the double-valued stability boundaries found for larger η (CP), the existence of multiple values of Ta_{crit} for some range of Re at fixed μ and η does not correspond to one base flow becoming unstable at several different Taylor numbers. Rather, it should be interpreted in terms of a base flow with a particular axial velocity (depending only on η) becoming unstable at two different magnitudes of the azimuthal velocity (whose profile depends only on μ and η), whose magnitude depends on Ta/Re.

Figure 4(b) shows that as Re increases, m_{crit} again increases from 0 to 1 (at point B), and from 1 to 2 (at point A) over the range of Re considered. Comparison to the $\mu = 0$ case (figures 1a and 1b) shows that these transitions occur at similar Reynolds numbers, and that the intermediate-Ta branch AC for $\mu = -0.25$ corresponds to the $m = 2$ branch in figure 1(a), which begins at A and continues to large Re.

Figure 4(c) shows that k_{crit} is again a piecewise continuous function of Re, which in this case is triple-valued for Reynolds numbers between the turning point C and the junction A. Unlike the behaviour observed for $\mu = 0$, the dependence of k_{crit} on Re is not fan-like. On the high-Ta branch, terminating at A, k_{crit} is essentially independent of Re, with a small discontinuity at B/B', where m_{crit} increases from 0 to 1. (The prime denotes a second point on the m_{crit}, k_{crit} or c_{crit} plots, at the same Re as the unprimed point, corresponding to a value of Re at which m_{crit} jumps.). The critical value of k is much smaller on the intermediate- and low-Ta branches, and increases on the former branch as Re decreases from the junction A to the turning point C. At some Re beyond C, k_{crit} reaches a maximum, and falls off nearly inversely with Re above about $Re = 200$.

Figure 4(d) and the enlargement figure 4(e) show that for $\mu = -0.25$, c_{crit} is positive and essentially constant on the $m = 0$ portion of the high-Ta branch, as in the $\mu = 0$ case considered above (figure 1d) and in all of the $\mu < \eta^2$ cases considered in CP and CRP for $\eta \geqslant 0.5$. The critical wave speed increases by approximately a factor of two at the first azimuthal wavenumber transition (B/B'), and then decreases monotonically until the junction is reached at A. At that point, c_{crit} jumps discontinuously to a negative value (about -32) at A', corresponding to a travelling-wave disturbance propagating upstream against the axial component of the base flow. As we move down along the intermediate branch of the stability boundary in figure 4(a), the magnitude of c_{crit} rapidly decreases, corresponding to a reduction in the speed of the backward-propagating neutral disturbance as Re decreases. At the turning point C, $c_{crit} = -3.59$. As Re increases on the low-Ta branch, c_{crit} continues to increase, and near $Re = 201$ smoothly passes through zero, corresponding to a reversal in direction of the travelling-wave disturbance, and the existence of a single Re at which the disturbance is stationary. Finally, as Re increases beyond 300, c_{crit} approaches its asymptotic value of about 0.1.

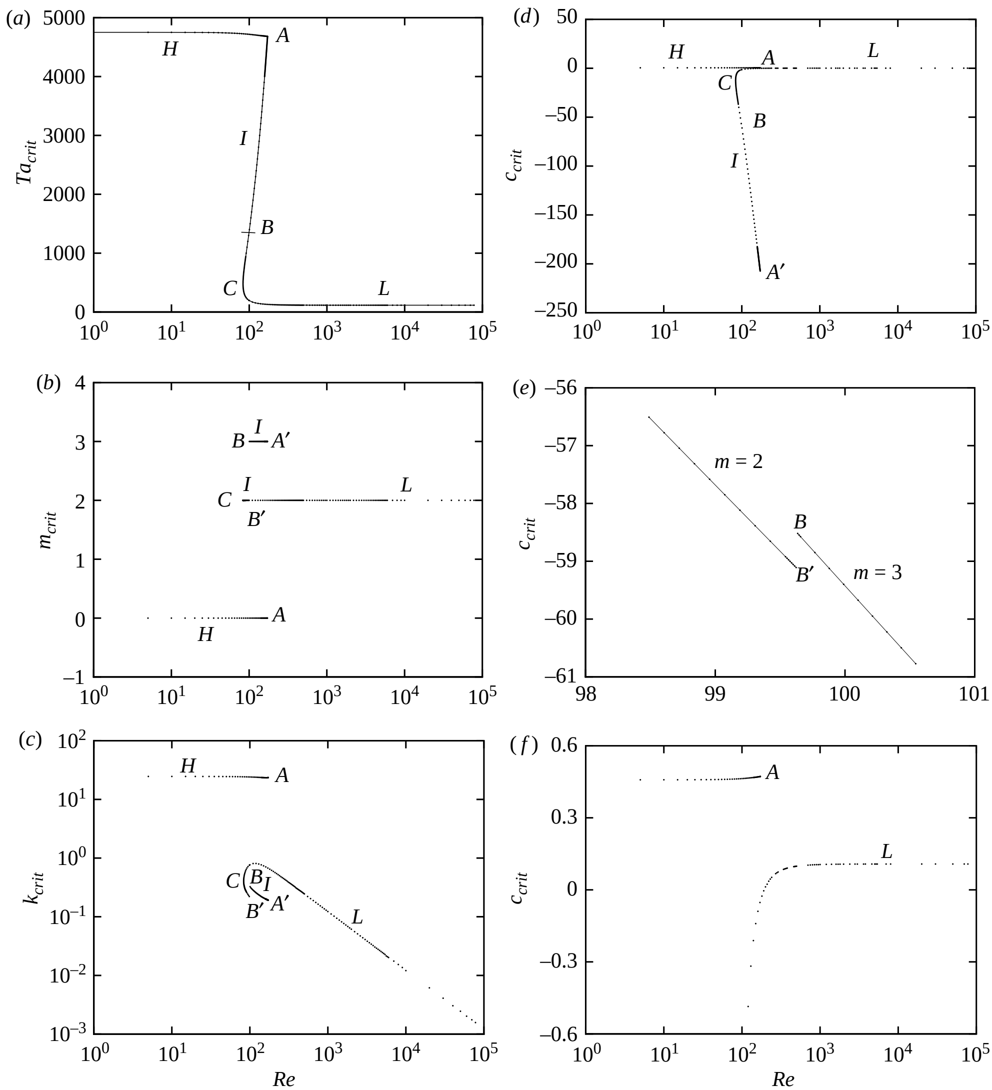

FIGURE 5. For $\mu = -0.5$ and $\eta = 0.1$: (*a*) critical *Ta*, (*b*) critical *m*, (*c*) critical *k*, (*d*) critical *c* versus *Re*, (*e*) critical *c* versus *Re* near the mode transition *B*, (*f*) critical *c* versus *Re* near $c_{crit} = 0$.

$\mu = -0.5$

For the counter-rotating $\mu = -0.5$ case, figure 5(*a*) shows that the high-*Ta* branch (H) of the stability boundary originates at $Re = 0$ and terminates near $Re = 172.0$ (point *A*), where it joins the intermediate-*Ta* branch (I) with a slope discontinuity. As we move downward on the intermediate branch, *Re* decreases, through a small slope discontinuity at point *B* (see figure 5*e*), to the turning point *C*, where this branch smoothly connects to the low-*Ta* (high-*Re*) branch near $Re = 83.3$. Thus, in the multi-valued range $83.3 \leqslant Re \leqslant 172.0$, the base flow is linearly stable below the low-*Ta* branch, as well as between the intermediate- and high-*Ta* branches. The flow is unstable between the low- and intermediate-*Ta* branches, and above the high-*Ta* branch.

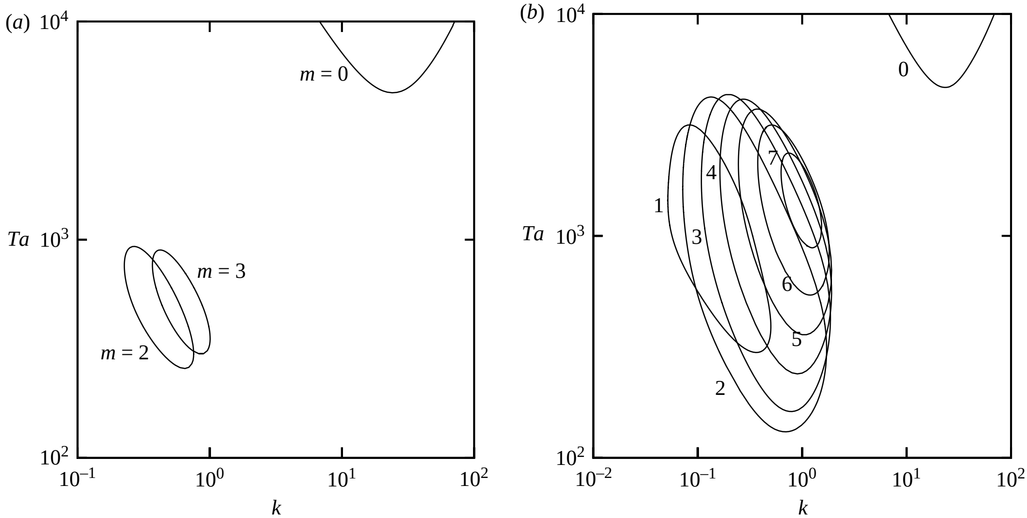

FIGURE 6. (a) Neutral curves for $Re = 90$, $\mu = -0.5$ and $\eta = 0.1$. (b) Neutral curves for $Re = 165$, $\mu = -0.5$ and $\eta = 0.1$, corresponding to azimuthal wavenumbers shown to the left of each curve.

For two values of Re in the triple-valued range, the neutral curves in figures 6(a) and 6(b) show that a gap exists between the maximum Ta on the CDNCs and the minimum Ta on the $m = 0$ neutral curve, which is the lowest-lying primary neutral curve (with a vertical asymptote at $k = 0$, and apparently existing as $k \to \infty$) for these Reynolds numbers. For $Re = 90$, figure 6(a) shows two CDNCs, lying at axial wavenumbers less than one-twentieth the value assumed by k at the minimum of the $m = 0$ neutral curve. As Re increases through 83.3, the $m = 2$ CDNC initially appears as a point, and at a slightly higher Re is joined by the $m = 3$ CDNC, which also makes its first appearance at a point. The flow is also stable for Ta below the minimum of the $m = 2$ CDNC. For $Re = 165$, figure 6(b) shows that several other CDNCs have appeared, and the gap between the minimum Ta on the $m = 0$ neutral curve and the largest Ta on any CDNC (on $m = 3$) has been greatly reduced. For $Re = 165$, the minimum still occurs on the $m = 2$ CDNC. (For $Re = 90$ and 165, all of the CDNCs and the $m = 0$ primary neutral curve are shown, and no part of any other neutral curve lies below the minimum of the $m = 0$ curve.).

The junction at point A corresponds to the Re (172.0) at which the gap disappears between the maximum on the $m = 3$ CDNC and the minimum on the $m = 0$ primary neutral curve. As we continue down the intermediate branch (I) of the stability boundary in figure 5(a), m_{crit} jumps from 3 to 2 at point B ($Re = 99.5$ in figure 5b), between the values of Re for which neutral curves are shown in figures 6(a) and 6(b), and each CDNC shrinks and ultimately coalesces at a point in the (k–Ta)-plane. The last of these coalescences (for the $m = 2$ CDNC at $Re = 83.3$) corresponds to the intermediate- and low-Ta branches of the Re–Ta stability boundary joining smoothly at the turning point C in figure 5(a), near $Ta = 480$. The behaviour of the neutral curves at each end of the triple-valued range is qualitatively identical to that found in earlier studies of the onset of buoyancy-driven convection in horizontal fluid layers (Pearlstein 1981; Pearlstein *et al.* 1989; Terrones & Pearlstein 1989; Lopez *et al.* 1990).

Figure 5(*b*) shows that $m_{crit} = 0$ on the high-*Ta* branch, jumping directly to 3 at point *A*. This value of m_{crit} is maintained as we move downward on the intermediate-*Ta* branch to *B*, at which point m_{crit} jumps to 2, which is the critical *m* up to at least $Re = 10^5$. For $\mu = -0.5$, there is no *Re* for which $m_{crit} = 1$. The maximum m_{crit} occurs at intermediate *Re* values, which differs from the $\mu = 0$ and -0.25 cases above and the $\mu < \eta^2$ cases considered for $\eta \geqslant 0.5$ in CP and CRP, for which m_{crit} increased by unit steps along the arclength of the stability boundary.

Figure 5(*c*) shows that k_{crit} is a piecewise continuous function of *Re*, and is triple-valued for Reynolds numbers between the turning point *C* near $Re = 83.3$ and the junction *A* near $Re = 172.0$. Like the behaviour predicted for $\mu = -0.25$, the dependence of k_{crit} on *Re* is not 'fan-like'. On the high-*Ta*, $m = 0$ branch, terminating at *A*, k_{crit} is essentially independent of *Re*. On the intermediate branch, k_{crit} increases as *Re* decreases from *A* to *B*. At *B*, where m_{crit} jumps from 3 to 2, k_{crit} decreases discontinuously and then increases through the turning point *C*, until reaching a maximum on the low-*Ta* branch near $Re = 120$. Beyond $Re = 120$, k_{crit} again varies nearly inversely with *Re*.

Figure 5(*d*) shows that on the high-*Ta* branch, c_{crit} is positive and essentially constant, as in the $\mu = 0$ and -0.25 cases considered above (figures 1*d* and 4*d*) and all $\mu > \eta^2$ cases considered in CP and CRP. The high-*Ta* branch emanating from $Re = 0$ terminates at *A*, and c_{crit} jumps discontinuously to a negative value at A' on the intermediate branch, as for $\mu = -0.25$. As we move down along the intermediate branch of the stability boundary toward *B* in figure 5(*a*), the magnitude of c_{crit} rapidly decreases, corresponding to a neutral disturbance propagating less rapidly upstream against the base flow as *Re* decreases. After a small discontinuity at *B* (see figure 5*e*) corresponding to m_{crit} jumping from 3 to 2, c_{crit} continues to increase as *Re* decreases on the intermediate-*Ta* branch. Near $Re = 192$, figure 5(*f*) shows that c_{crit} changes sign, corresponding to a reversal in direction of the travelling-wave disturbance, and the existence of a single *Re* at which the disturbance is stationary. Finally, as *Re* increases beyond 300, c_{crit} approaches its asymptotic value of about 0.1.

$\mu = -1$

For $\mu = -1$, figure 7(*a*) shows that Ta_{crit} is single-valued and decreases monotonically over $0 \leqslant Re \leqslant 79$ from its $Re = 0$ value of 9414.4. For $79 < Re < 305$, there again exist three values of Ta_{crit} and two disjoint ranges of stable *Ta*, one below the low-*Ta* branch and one between the intermediate- and high-*Ta* branches. As for $\mu = -0.25$ and -0.5, a slope discontinuity occurs where the intermediate- and high-*Ta* branches join near the junction at $Re = 305$ (point *A*), corresponding to a jump in m_{crit} from 1 to 3. The connection between the intermediate- and low-*Ta* branches at the turning point *C* near $Re = 79$ is smooth, since there is no jump in m_{crit}. At *B*, m_{crit} jumps to 2, which value persists until at least $Re = 10^5$. For large *Re*, Ta_{crit} is single-valued and approaches its asymptotic value ($Ta_{crit}^{\infty} \approx 56$). We note that the range of *Re* for which multiple critical Taylor numbers exist is larger than for $\mu = -0.25$ or -0.5.

For $\mu = -1$, figure 7(*b*) shows that over the entire range $0 \leqslant Re < 4 \times 10^4$, there is no *Re* for which $m_{crit} = 0$, unlike the $\mu = 0$, -0.25 and -0.5 cases, so that there is no *Re* for which the onset of instability occurs through an axisymmetric disturbance.

The dependence of k_{crit} on *Re* (figure 7*c*) differs from that for less negative values of μ, since m_{crit} is constant on the intermediate-*Ta* branch, and jumps at B, below

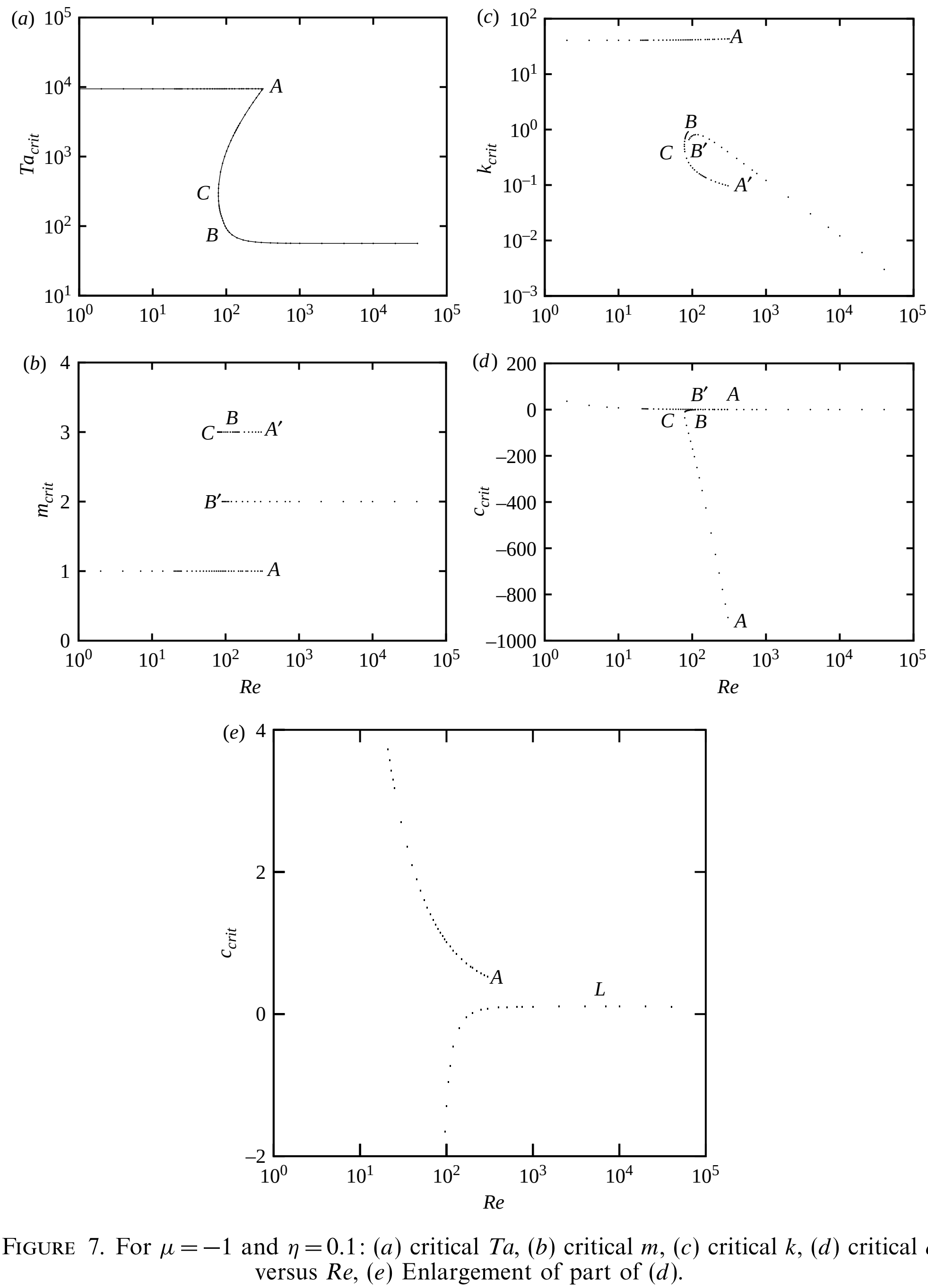

FIGURE 7. For $\mu = -1$ and $\eta = 0.1$: (*a*) critical Ta, (*b*) critical m, (*c*) critical k, (*d*) critical c versus Re, (*e*) Enlargement of part of (*d*).

the turning point. Again, there is a nearly inverse dependence of k_{crit} on Re at large Reynolds number. On a scale capturing its overall variation, the dependence of c_{crit} on Re shown in figure 7(*d*) appears to be similar to that for $\mu = -0.5$ in figure 5(*d*). Closer examination of the region near the junction (A) between the intermediate- and high-Ta branches, however, shows that as the junction is approached from the intermediate branch, c_{crit} decreases for $\mu=-1$ (figure 7*e*) and increases for $\mu=-0.5$ (figure 5*f*).

2.3. *Co-rotating cylinders* ($\mu=0.2$)

We here consider the co-rotating case $\mu=0.2$, investigated for $\eta=0.5$ experimentally and computationally by Takeuchi & Jankowski (1981) for Re up to 150 and 100, respectively, and computationally by CP up to $Re_{AP}=10\,359$. For $\mu=0.2$ and $\eta=0.1$, the $Re=0$ Couette flow is linearly stable according to the $\mu>\eta^2$ criterion (Synge 1938), and the stability boundary cannot intersect the $Re=0$ axis. The results differ qualitatively from those shown above for $\mu<\eta^2$, as well as from those of CP for $\mu=\eta=0.5$.

For $\mu=0.2$, figure 8(*a*) shows that up to about $Re=66.8$, the flow is stable for all Ta, which differs from the stability boundaries for $\mu\leqslant 0$ (figures 1*a*, 4*a*, 5*a* and 7*a*), in which for small Re, SPF is stable for only a finite range of Ta. For $Re>66.8$, the stability boundary has two branches, and there are two disjoint ranges of stable Ta, the first being finite and lying below the low-Ta branch, and the second being semi-infinite and lying above the high-Ta branch. As Re increases on the low-Ta branch from the turning point near $Re=66.8$, Ta_{crit} monotonically decreases to its asymptotic value ($Ta^{\infty}_{crit}\approx 241$), while on the high-$Ta$ branch, Ta_{crit} continues to increase with Re up to at least $Re=10^3$. This behaviour contrasts to the single branch found for large Re when $\eta=0.1$ and $\mu\leqslant 0$, on which Ta_{crit} approaches an asymptote as $Re\to\infty$. The asymptotic behaviour on the lower branch as $Re\to\infty$ contrasts to that for $\eta\geqslant 0.5$ (CP and CRP), in which cases Ta_{crit} vanishes at a finite Re_{AP}.

Figure 8(*b*) shows that $m_{crit}=-3$ at the turning point and on both branches for sufficiently small Re. On the low-Ta branch, m_{crit} jumps to -2 near $Re=105$, and remains unchanged at larger Re. On the high-Ta branch, m_{crit} falls to -4 near $Re=162$, and to -5 near $Re=622$. For $\mu=0.2$, there is no value of Re for which the onset of instability occurs through an axisymmetric disturbance. The exclusively negative values of m_{crit} correspond to vortices propagating with a helical sense, relative to the axial flow and inner cylinder rotation, opposite to that for disturbances having $m_{crit}>0$, and have been found previously only for $\mu=\eta=0.5$, for which μ also exceeds η^2.

Figure 8(*c*) shows that as Re decreases on the low-Ta branch, k_{crit} increases like $1/Re$, as for the other μ values considered. At point B, where m_{crit} jumps from -2 to -3 as Re decreases, k_{crit} increases discontinuously. As Re decreases towards the turning point, k_{crit} passes through a maximum, and then decreases continuously through the turning point until m_{crit} jumps from -3 to -4 at point A on the high-Ta branch. Beyond point A, k_{crit} decreases monotonically with increasing Re in each range of Re for which m_{crit} is constant, with a discontinuous increase each time m_{crit} jumps. We note that the critical wavenumbers for the high- and low-Ta branches intersect at point E near $Re=520$, and that this intersection corresponds to two different values of Ta_{crit} and two different values of m_{crit}.

For $\mu=0.2$, figures 8(*d*) and 8(*e*) show that at large Re on the low-Ta branch, c_{crit} is positive. As Re approaches the turning point ($Re\approx 66.8$) along the $m_{crit}=-2$ low-Ta branch, c_{crit} decreases, passing smoothly through zero near $Re=160$. The critical wave speed continues to decrease as we move through the turning point, with the fall-off being nearly linear in log Re as Re increases along the high-Ta branch. The discontinuities of c_{crit} at the Reynolds numbers where m_{crit} jumps are barely discernible on the scale of figure 8(*d*).

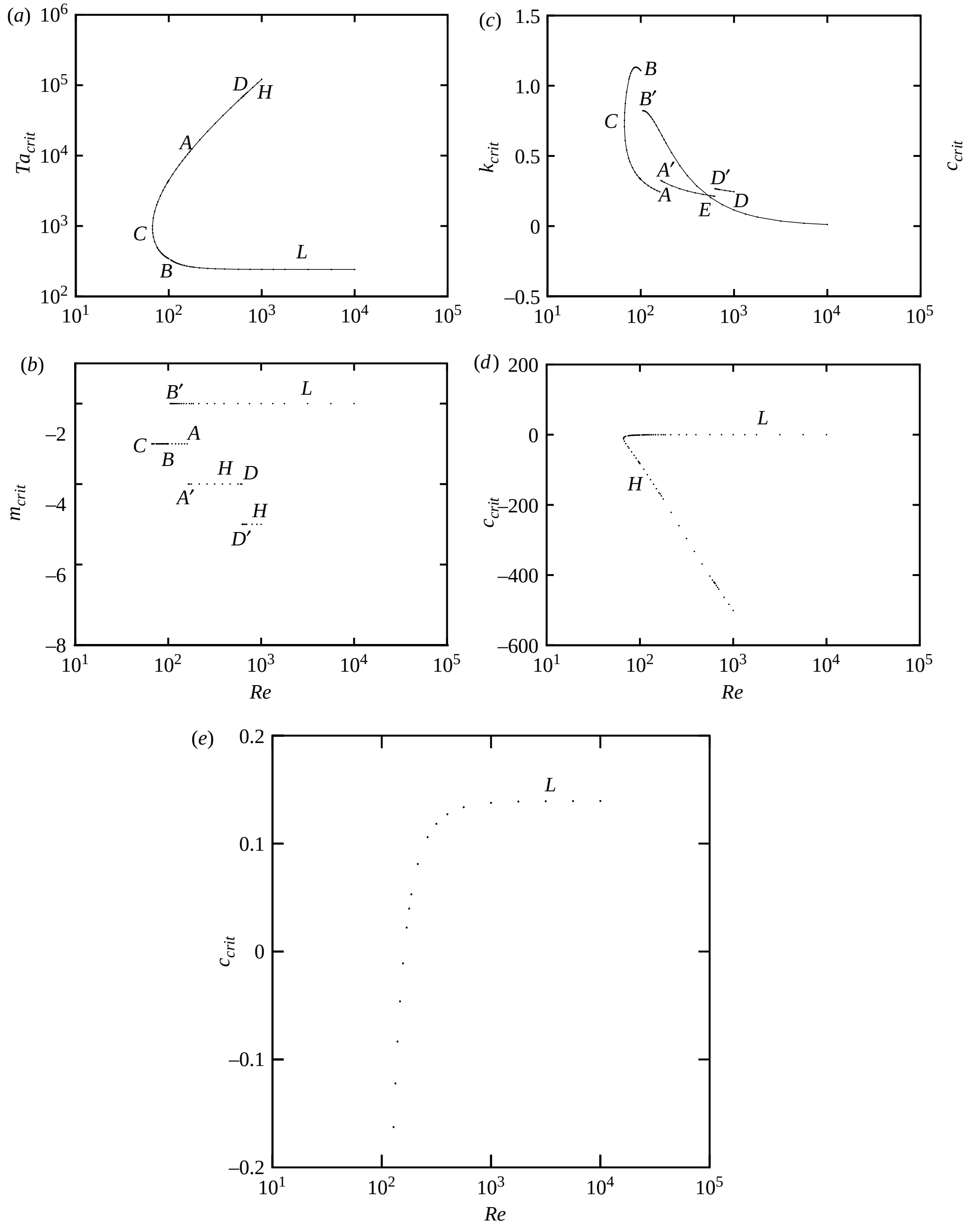

FIGURE 8. For $\mu = 0.2$ and $\eta = 0.1$: (*a*) critical *Ta*, (*b*) critical *m*, (*c*) critical *k*, (*d*) critical *c* versus *Re*, (*e*) Enlargement of part of (*d*).

3. Discussion

3.1. *Relationship to other work*

For spiral Poiseuille flow with $\eta = 0.1$, the only previous results appear to be those of Chung & Astill (1977), Hasoon & Martin (1977), and Recktenwald *et al.* (1993), all for $\mu = 0$. Chung & Astill showed critical values of *Ta* (their figure 5) for $Re = 0$, 50 and 100, and stated that $m_{crit} = 0$ for $Re \leqslant 100$. For $\eta = 0.1$, the Taylor number defined by them is exactly one-ninth of our Ta, and their critical value at $Re = 0$ corresponds to $Ta_{crit} \approx 3 \times 10^4$, more than twenty times the value we have computed. At $Re = 0$, our value $Ta_{crit} = 1264.43$ is in excellent agreement with that of Walowit, Tsao & DiPrima (1964), to whose work Chung & Astill made no comparison or reference. Errors in the results of Chung & Astill at larger η have been discussed by Takeuchi & Jankowski (1981) and Ng & Turner (1982). The computations of Hasoon & Martin (1977), which predict that Ta_{crit} increases monotonically with Re over the range $0 \leqslant Re < 1000$, are in disagreement with the results shown in figure 1(a). How much of the discrepancy is due to use of a uniform axial velocity profile by Hasoon & Martin, and how much is attributable to an error in their governing equations (DiPrima & Pridor 1979), is not known.

For several values of η, Recktenwald *et al.* used a shooting method to compute the onset of instability with respect to axisymmetric disturbances for $Re = 0, 1, 2, \ldots, 20$, and fitted the results to a polynomial over that range, which in our notation takes the form

$$Ta_{crit} = Ta^0_{crit}[1 + (Re/a_2)^2 + (Re/a_4)^4]^{1/2}, \tag{3.1}$$

where Ta^0_{crit}, a_2 and a_4 were determined by a least-squares fit. As shown in § 2.1, the critical disturbance for $\mu = 0$ and $\eta = 0.1$ is indeed axisymmetric up to $Re = 46$. The agreement between the approximation (3.1) and our computations is better than 6 parts per million at $Re = 0, 1, 2, \ldots, 19$, and 14 parts per million at $Re = 20$, suggesting the correctness of both sets of results. Comparison of (3.1) to our numerical results shows that the difference is less than 0.3 % at $Re = 40$, a value twice the highest Re for which Recktenwald *et al.* computed results used to determine the coefficients in the fitted form (3.1). Good agreement also obtains between our computed values of k_{crit} and the fitted form of the critical wavenumber

$$k_{crit} = 3.3393 - (Re/133.1)^2 + (Re/74.76)^4, \tag{3.2}$$

with a root-mean-square (r.m.s.) difference of 7×10^{-5} for $Re = 1, 2, \ldots, 20$. (The form $k_{crit} = 3.3393[1 - (Re/133.1)^2 + (Re/74.76)^4]$ given by Recktenwald *et al.* has an r.m.s. error 300 times larger. For $\eta = 0.5$, however, the functional form for k_{crit} given by Recktenwald *et al.* fits our results very well, and is a much better fit than the analogue of (3.2).) The r.m.s. difference between our computed wave speeds and the values of Recktenwald *et al.* (using (3.2) instead of the expression given by them for k_{crit}) is 2.4×10^{-4} for the same values of Re. The Re range considered by Recktenwald *et al.* was too small for the qualitative differences between results for $\eta = 0.1$ and the larger values of η investigated by those authors to be apparent.

The results shown in table 1 and extrapolated in § 2.1 strongly suggest that for annular Poiseuille flow (i.e. absent rotation), no linear instability occurs for $0 < \eta < \hat{\eta} \approx 0.115$. These results are consistent with the earlier computational work of Mahadevan & Lilley (1977) and Garg (1980), who showed that the critical Re increased rapidly as η approached 0.15 from above. Although the relationship of the stability of narrow-gap ($\eta \rightarrow 1$) annular Poiseuille flow to the stability of plane Poiseuille flow has been discussed (Mott & Joseph 1968; Mahadevan & Lilley 1977; Garg 1980; Landau & Lifshitz 1987; Sadeghi & Higgins 1991), and the linear stability of circular Poiseuille flow at all Re has been identified as representing a 'limit result' for the axial profiles as $\eta \rightarrow 0$ in annular Poiseuille flow (Mott & Joseph 1968), we are aware of no previous discussion connecting the lack of a critical Re for circular Poiseuille flow to the lack of a critical Re for small-η annular Poiseuille flow. Existence of a vertical asymptote at non-zero $\hat{\eta}$ shows that the apparent linear stability of circular Poiseuille flow ($\eta = 0$) at all Re (Salwen, Cotton & Grosch 1980) is not an isolated case, and that Poiseuille flow is linearly stable for all Re from $\eta = 0$ (for circular Poiseuille flow) up to $\eta = \hat{\eta} \approx 0.115$ (for annular Poiseuille flow). Such a result is inconsistent with the statement (Landau & Lifshitz 1987) that 'There appears to be a critical R_{cr} for all non-zero values $R_1 < R_2 < 1$; when $R_1/R_2 \to 0$, $R_{cr} \to \infty$', where R_{cr} is the critical Reynolds number and R_1 and R_2 correspond to our R_i and R_o, respectively. (We thank an anonymous reviewer for comments that ultimately led us to this passage.)

Finally, for $\mu = 0$, the ηTa versus Re curves in figure 2 show that the stability boundary for $\eta = 0.1$ has a high-Re asymptote very close to the plateau values for the larger-η cases considered in CP and CRP. As for $\eta = 0.5$, the $\eta = 0.1$ stability boundary has a global maximum at an Re at which transition occurs between critical values of m. Unlike the $\eta = 0.5$ case, the results for $\eta = 0.1$ show that Ta_{crit} on the high-Re plateau lies below the $Re = 0$ value for Taylor–Couette flow. That the ηTa scaling in figure 2 nearly 'collapses' the plateau behaviour for $0.1 \leqslant \eta \leqslant 0.95$ shows that for a wide range of Re and η, the critical angular velocity of the inner cylinder (with the outer cylinder fixed) is given by $\omega_{crit} = 44.7\nu/R_i R_o$, accurate within 3 %.

3.2. *Direction of wave propagation*

In the first analysis of the stability of SPF, which considered zero and non-zero rotation rate ratios μ, Goldstein (1937) asserted that 'when there is flow parallel to the axis, no steady disturbance is possible'. This is consistent with the results of the linear stability analysis for $\mu \geqslant 0$, and for all μ considered for $\eta \geqslant 0.5$ in CP and CRP. For $\eta = 0.1$, however, figures 4(e), 6(f), and 8(e) show that for each counter-rotating case considered, c_{crit} passes smoothly through zero on the intermediate-Ta branch. Thus, for $\eta = 0.1$, the assertion of Goldstein is consistent with the linear stability analysis except at one Re. Linear stability theory thus predicts that there is a single Reynolds number Re_s for which we can decrease Ta from the stable range between the intermediate- and high-Ta branches, and transition from a steady axisymmetric z-invariant SPF base flow to more complicated flow through a steady non-axisymmetric axially-periodic disturbance. For Re slightly less than Re_s, the direction of propagation of the disturbance flow would be upstream against the axial component of the base flow, while for Re slightly greater than Re_s, the disturbance structure will propagate downstream. We note that for $\mu = 0$ and $\eta = 0.8$, the experimental work of Bühler & Polifke (1990) shows that the direction of propagation of axially travelling waves with $m = 1$ can be reversed by changing Re.

Our prediction of a single Re at which the onset frequency is zero for neutral disturbances of infinitesimal amplitude with $\eta = 0.1$ can be contrasted to experiments for larger η in which steady helical vortices exist for a range of conditions (Bühler & Polifke 1990; Lueptow, Docter & Min 1992; Tsameret & Steinberg 1994). We also note that for six small values of Re ($0.11 \leqslant Re \leqslant 1.15$) and $\eta = 0.677$, figure 16 of Giordano *et al.* (1998) shows that the dimensionless axial phase velocity, $V_{phase}/\overline{V}_Z$ (which is our c_{crit} at $Ta = Ta_{crit}$), decreases nearly linearly to zero with increasing Ta in some range above Ta_{crit}. For at least one Reynolds number, their data suggest that V_{phase} remains zero over some range of Ta beyond the Ta at which V_{phase} first vanishes.

3.3. *Implications for experiment*

For $\eta = 0.5$ and $\mu > \eta^2$, multi-valued *Re*–*Ta* stability boundaries for SPF have been predicted by Meseguer & Marques (2002) with μTa fixed, and by CP with μ fixed. As shown by the latter authors, the results of Meseguer & Marques (2002) are incorrect, owing to restriction of the disturbances to an insufficient range of azimuthal wavenumbers. For fixed values of $\mu \neq 1$, the multi-valued stability boundaries found for $\eta = 0.5$ (CP) are double-valued in the *Re*–*Ta* plane for $Re > Re_{min} > 0$. For $\mu > \eta^2$ and $0 \leqslant Re < Re_{min}$, SPF is linearly stable for all *Ta*. As *Re* increases through the turning point at Re_{min}, closed neutral curves emerge from points in the *k*–*Ta* plane. The work of CP shows that for $\eta = 0.5$ and several rotation rate ratios $\mu > \eta^2$, SPF is unstable in the range between the lowest *Ta* on any of these neutral curves and the highest *Ta* on any of them, and linearly stable for *Ta* lying above or below this range. For the cases considered, the upper and lower limits of the unstable range corresponded to negative and positive values of the azimuthal wavenumber *m*, respectively.

For $\eta = 0.1$ and $\mu = 0.2 > \eta^2$, the multi-valued stability boundary differs from that found by CP in that there is no finite *Re* at which a transition from centrifugal instability to Tollmien–Schlichting-like instability occurs, with non-rotating annular Poiseuille flow being linearly stable at all *Re*. There is still a turning point Re_{min} below which SPF is linearly stable at all *Ta*, and above which instability occurs only in a finite range of *Re*. On the other hand, for $\eta = 0.1$ and $\mu < 0$, the results in § 2.2 show that the stability boundary extends over the entire range of *Re*, and is triple-valued in a finite range of *Re*. In that range of *Re*, SPF is stable below the lowest critical *Ta* and between the intermediate and highest critical *Ta*, and unstable for all other *Ta*.

We are thus led to consider experiments to investigate the triple-valued stability boundaries predicted for $\eta = 0.1$ and $\mu < 0$, with the goal of determining if SPF is indeed realizable in the two disjoint ranges of stable *Ta* predicted over a range of *Re*. For SPF with $\eta = 0.1$, figures 4(*a*), 5(*a*) and 7(*a*) show that for each counter-rotating case considered, there are three critical values of *Ta* for $Re_1(\mu) \leqslant Re \leqslant Re_2(\mu)$, where Re_1 and Re_2 denote the minimum and maximum values of *Re* for which multiplicity is predicted. We denote the values of *Ta* on the low-, intermediate- and high-*Ta* branches by Ta_L, Ta_I and Ta_H, respectively. As discussed in § 2.2, the analysis predicts that in the multi-valued range of *Re*, SPF is linearly stable for $Ta \leqslant Ta_L$ and for $Ta_I \leqslant Ta \leqslant Ta_H$, and unstable for $Ta_L \leqslant Ta \leqslant Ta_I$ and $Ta \geqslant Ta_H$. We note that Re_1 and Re_2 increase and decrease, respectively, as μ increases, with the width, $Re_2 - Re_1$, of the range being 221, 89 and 32 for $\mu = -1$, -0.5 and -0.25, respectively. Comparison of figures 1(*a*) and 4(*a*) shows that there is a negative value of μ (denoted by μ_-) at which the slope of the Re–Ta_{crit} plot is infinite, and that in the range $\mu_- < \mu \leqslant 0$ there is no *Re* for which the stability boundary is multi-valued. From our results, we see that $-0.25 < \mu_- < 0$ for $\eta = 0.1$. On the other hand, we know from the work of Synge (1938) that the $Re = 0$ base flow is linearly stable for $\mu > \eta^2 = 0.01$, which suggests that at $Re = 0$, Ta_{crit} grows without bound as $\mu \rightarrow \eta^2$ from below.

For $\mu < \mu_-$, the stability boundaries shown in figures 4(*a*), 5(*a*) and 7(*a*) suggest that for $Re_1(\mu) \leqslant \widetilde{Re} \leqslant Re_2(\mu)$, the three critical values of *Ta* might be found experimentally as follows. The lowest value, Ta_L, might be reached by increasing *Re* at $Ta = 0$ until reaching $\widetilde{Re}$, and then increasing *Ta* at fixed *Re* until Ta_L is reached. The intermediate and upper Taylor numbers, Ta_I and Ta_H, respectively, might be reached by starting at a Taylor number in the range $Ta_I \leqslant Ta \leqslant Ta_H$ at $Re = 0$, and increasing *Re* to $\widetilde{Re}$. Then *Ta* could be increased until Ta_L is reached, or decreased until Ta_I is reached.

A key issue in determining if SPF becomes unstable as predicted by linear analysis in the range of multi-valuedness is whether instability can set in through disturbances of finite amplitude in one or both ranges of stable Ta. We first consider $\mu < \mu_-$ and the possibility of reaching Ta_L. For the cases considered, the computed values of Re_2 (all less than about 300) are not very large, so that there is a reasonable expectation that the non-rotating annular Poiseuille flow is either globally stable, or at least stable with respect to a large class of finite-amplitude disturbances. This expectation is based on the fact that plane Poiseuille flow, the narrow-gap limit ($\eta \to 1$) of annular Poiseuille flow, is globally stable up to about 1000 (Carlson, Widnall & Peeters 1982), while for $\eta = 0$, global stability obtains for Re up to about 2000. This suggests that annular Poiseuille flow should be experimentally realizable at the required values of Re for $Ta = 0$. Furthermore, the excellent agreement between our computations and the experimental results of Snyder (1965) and Mavec (1973) detailed in CRP clearly shows that for $\eta = 0.77$ and $\eta \approx 0.95$, there is a wide range of Re and μ for which finite-amplitude disturbances in a linearly stable flow either do not grow, or grow only in a very narrow range of stable Ta just below the linear Ta_{crit}. Those comparisons are consistent with the conclusion of Takeuchi & Jankowski (1981) that finite-amplitude instability does not occur for $Re \leqslant 40$ when $\mu = 0$ and $\eta = 0.5$.

For $\eta = 0.1$ and each negative μ considered, our analysis predicts that as $Re \to \infty$, SPF is linearly stable for $0 \leqslant Ta < Ta^{\infty}_{crit}$. Thus, for sufficiently large Re, additional axial shear apparently has no effect on the onset of centrifugal instability via infinitesimal disturbances. Moreover, figure 2 strongly suggests that the value of Re^* at which the transition from centrifugal to Tollmien–Schlichting-like instability occurs (see CP) increases without bound as $\eta \to \hat{\eta}$ from above, corresponding to the disappearance of linear instability in annular Poiseuille flow at $\hat{\eta}$. Computations reported in § 2.1 suggest the existence, for $\eta < \hat{\eta}$ and $\mu < 0$, of an η- and μ-dependent Ta^{∞}_{crit} such that SPF is linearly stable for all Re if $Ta < Ta^{\infty}_{crit}$, and unstable for sufficiently large Re if $Ta > Ta^{\infty}_{crit}$.

For $\eta = 0.1$ and $\mu = 0$ and -0.25, it is clear from the Re–Ta_{crit} plots (figures 1(a) and 4(a), respectively) that development of a multi-valued Re–Ta_{crit} stability boundary originates with the $m_{crit} = 2$ branch assuming an infinite slope at point A, where the transition from $m_{crit} = 1$ to $m_{crit} = 2$ occurs as Re increases. As we approache from below the rotation rate ratio μ_- at which multi-valuedness sets in, the slope of the $m_{crit} = 2$ branch must become infinite and the width of the range of multiplicity must vanish (i.e. $Re_2 - Re_1 = 0$). The dependence of μ_- on η as $\eta \to \hat{\eta}$ from below is not clear.

4. Conclusions

The linear stability of spiral Poiseuille flow for $\eta = 0.1$ is quite different from that for $\eta \geqslant 0.5$. One key difference is the absence of a transition from centrifugal to Tollmien–Schlichting-like instability at high Re. For $\eta = 0.1$, there is no critical Re beyond which the non-rotating flow is unstable. In fact, for $\eta < \hat{\eta} \approx 0.115$ there is no linear instability, so that like circular Poiseuille flow, annular Poiseuille flow for $\eta < \hat{\eta}$ is linearly stable for all Re. Thus, for $\eta < \hat{\eta} \approx 0.115$, SPF is linearly stable below a rotation rate-dependent asymptotic value $Ta^{\infty}_{crit}(\mu)$ as $Re \to \infty$.

In addition, for $\eta = 0.1$ and each rotation rate ratio considered, we find a range of Re for which closed disconnected neutral curves exist in the k–Ta plane. For each negative μ, these neutral curves give rise to a triple-valued Re–Ta stability boundary over some range of Re, corresponding to two disjoint ranges of stable rotation rates and two disjoint ranges of unstable rotation rates. This contrasts to the results for larger η, where no multi-valuedness was found for $\mu < \eta^2$. For $\mu > \eta^2$, there is a finite range of *Re* beginning at 0 in which the flow is linearly stable for all *Ta*, and a semi-infinite range of *Re* in which a double-valued stability boundary separates two disjoint ranges of stable rotation rates. For each case considered in which the outer cylinder rotates, there is a single non-zero *Re* at which the axial wave speed of the critical disturbance vanishes, corresponding to a reversal of the axial direction of the propagating disturbance.

This work was supported in part by NSF Grants CTS-9422770 and CTS-9613241, and DOE Grant DE-FG02-96ER45607. Some of the computations were performed using the facilities of the National Center for Supercomputing Applications. D. L. C. gratefully acknowledges support of a National Research Council Postdoctoral Fellowship during revision of the manuscript.

REFERENCES

Ali, M. & Weidman, P. D. 1990 On the stability of circular Couette flow with radial heating. *J. Fluid Mech.* **220**, 53–84.

Blennerhassett, P. J. 1980 On the generation of waves by wind. *Phil. Trans. R. Soc. Lond.* A **298**, 451–494.

Bühler, K. & Polifke, N. 1990 Dynamical behaviour of Taylor vortices with superimposed axial flow. *Nonlinear Evolution of Spatio-Temporal Structures in Dissipative Continuous Systems* (ed. F. H. Busse & L. Kramer), pp. 21–29. Plenum Press, New York.

Carlson, D. R., Widnall, S. E. & Peeters, M. F. 1982 A flow-visualization study of transition in plane Poiseuille flow. *J. Fluid Mech.* **121**, 487–505.

Chen, Y. M. & Pearlstein, A. J. 1989 Stability of free-convection flows of variable-viscosity fluids in vertical and inclined slots. *J. Fluid Mech.* **198**, 513–541.

Chung, K. C. & Astill, K. N. 1977 Hydrodynamic instability of viscous flow between coaxial cylinders with fully developed axial flow. *J. Fluid Mech.* **81**, 641–655.

Cotrell, D. L., Rani, S. L. & Pearlstein, A. J. 2004 Computational assessment of subcritical instability and delayed onset in spiral Poiseuille flow experiments. *J. Fluid Mech.* **509**, 353–378.

Cotrell, D. L. & Pearlstein, A. J. 2004 The connection between centrifugal instability and Tollmien–Schlichting-like instability for spiral Poiseuille flow. *J. Fluid Mech.* **509**, 331–351.

Debler, W., Füner, E. & Schaaf, B. 1969 Torque and flow patterns in supercritical circular Couette flow *Proc. 12th Intl Congress Appl. Mech.* (ed. M. Hetenyi and W. G. Vincenti), pp. 158–178. Springer.

DiPrima, R. C., Eagles, P. M. & Ng, B. S. 1984 The effects of radius ratio on the stability of Couette flow and Taylor vortex flow. *Phys. Fluids* **27**, 2403–2411.

DiPrima, R. C. & Pridor, A. 1979 The stability of viscous flow between rotating concentric cylinders with an axial flow. *Proc. R. Soc. Lond.* A **366**, 555–573.

Garg, V. K. 1980 Spatial stability of concentric annular flow. *J. Phys. Soc. Japan* **49**, 1577–1583.

Giordano, R. C., Giordano, R. L. C., Prazeres, D. M. F. & Cooney, C. L. 1998 Analysis of a Taylor–Poiseuille vortex flow reactor—I: Flow patterns and mass transfer characteristics. *Chem. Engng Sci.* **53**, 3635–3652.

Goldstein, S. 1937 The stability of viscous fluid flow between rotating cylinders. *Proc. Camb. Phil. Soc.* **33**, 41–61.

Hasoon, M. A. & Martin, B. W. 1977 The stability of viscous axial flow in an annulus with a rotating inner cylinder. *Proc. R. Soc. Lond.* A **352**, 351–380.

Landau, L. D. & Lifshitz, E. M. 1987 *Fluid Mechanics*, 2nd ed. Pergamon.

Lopez, A. R., Romero, L. A. & Pearlstein, A. J. 1990 Effect of rigid boundaries on the onset of convective instability in a triply diffusive fluid layer. *Phys. Fluids* A **2**, 897–902.

Lueptow, R. M., Docter, A. & Min, K. 1992 Stability of axial flow in an annulus with a rotating inner cylinder. *Phys. Fluids* A **4**, 2446–2455.

Mahadevan, R. & Lilley, G. M. 1977 The stability of axial flow between concentric cylinders to asymmetric disturbances. *AGARD* CP-224, pp. 9-1–9-10.

Mavec, J. A. 1973 Spiral and toroidal secondary motions in swirling flows through an annulus at low Reynolds numbers. MS thesis, Illinois Inst. Tech., Chicago.

Meseguer, A. & Marques, F. 2002 On the competition between centrifugal and shear instability in spiral Poiseuille flow. *J. Fluid Mech.* **455**, 129–148.

Mott, J. E. & Joseph, D. D. 1968 Stability of parallel flow between concentric cylinders. *Phys. Fluids* **11**, 2065–2073.

Ng, B. S. & Turner, E. R. 1982 On the linear stability of spiral flow between rotating cylinders. *Proc. R. Soc. Lond.* A **382**, 83–102.

Pearlstein, A. J. 1981 Effect of rotation on the stability of a doubly diffusive fluid layer. *J. Fluid Mech.* **103**, 389–412.

Pearlstein, A. J., Harris, R. M. & Terrones, G. 1989 The onset of convective instability in a triply diffusive fluid layer. *J. Fluid Mech.* **202**, 443–465.

Recktenwald, A., Lücke, M. & Müller, H. W. 1993 Taylor vortex formation in axial through-flow: linear and weakly nonlinear analysis. *Phys. Rev.* E **48**, 4444–4454.

Resende, M. M., Tardioli, P. W., Fernandez, V. M., Ferreira, A. L. O., Giordano, R. L. C. & Giordano, R. C. 2001 Distribution of suspended particles in a Taylor–Poiseuille vortex flow reactor. *Chem. Engng Sci.* **56**, 755–761.

Sadeghi, V. M. & Higgins, B. G. 1991 Stability of sliding Couette–Poiseuille flow in an annulus subject to axisymmetric and asymmetric disturbances. *Phys. Fluids* **3**, 2092–2104.

Salwen, H., Cotton, F. W. & Grosch, C. E. 1980 Linear stability of Poiseuille flow in a circular pipe. *J. Fluid Mech.* **98**, 273–284.

Snyder, H. A. 1965 Experiments on the stability of two types of spiral flow. *Ann. Phys.* **31**, 292–313.

Snyder, H. A. 1970 Waveforms in rotating Couette flow. *Intl J. Non-Linear Mech.* **5**, 659–685.

Strong, A. B. & Carlucci, L. 1976 An experimental study of mass transfer in rotating Couette flow with low axial Reynolds number. *Can. J. Chem. Engng* **54**, 295–298.

Synge, J. L. 1938 On the stability of a viscous liquid between two rotating coaxial cylinders. *Proc. R. Soc. Lond.* A **167**, 250–256.

Takeuchi, D. I. & Jankowski, D. F. 1981 A numerical and experimental investigation of the stability of spiral Poiseuille flow. *J. Fluid Mech.* **102**, 101–126. Corrigendum **113**, 536 (1981).

Terrones, G. & Pearlstein, A. J. 1989 The onset of convection in a multicomponent fluid layer. *Phys. Fluids* A **1**, 845–853.

Tsameret, A. & Steinberg, V. 1994 Absolute and convective instabilities and noise-sustained structures in the Couette–Taylor system with an axial flow. *Phys. Rev.* E **49**, 1291–1308.

Walowit, J., Tsao, S. & DiPrima, R. C. 1964 Stability of flow between arbitrary spaced concentric cylindrical surfaces including the effect of radial temperature gradient. *J. Appl. Mech.* **31**, 585–593.